Competition Among fcc-Like, Double-Layered Flat, Tubular Cage, and Close-Packed Structural Motifs for Medium-Sized Au_n (n = 21−28) Clusters

Dongxu Tian*,†,§ and Jijun Zhao*,‡,§

Department of Chemistry, School of Chemical Engineering, State Key Laboratory of Materials Modification by Laser, Electron, and Ion Beams, School of Physics and Optoelectronic Technology, and College of Advanced Science and Technology, Dalian University of Technology, Dalian 116024, China

Received: August 27, 2007

Using density functional theory calculations, we compared four kinds of possible structural motifs of the medium-sized Au_n (n = 21−28) clusters, i.e., fcc-like, double-layered flat, tubular cage, and close-packed. Our results show strong competition between those structural motifs in the medium-sized gold clusters. Au_n (n = 21−23) adopt fcc-like structure owing to the high stability of tetrahedral Au_{20}. A structural transition from fcc-like to tubular occurs at Au_{24}, and the tubular motif continues at Au_{27} and Au_{28}. Meanwhile, a double-layered flat structure was found at Au_{25}, and a pyramid-based structure at Au_{26}. The relationship between electronic properties and cluster geometry was also discussed.

I. Introduction

Gold nanoclusters have been the focus of intensive studies owing to their importance in many fields such as catalysis, nanoelectronics, and biomedicine.[1,2,3] Because of the strong relativistic effect[4] and possible metal aromaticity,[5] previous theoretical and experimental studies revealed that Au_n clusters exhibit a variety of fascinating atomic structures, e.g., planar structures up to about n = 13,[6] double-layered flat configurations in the size range of n = 13−16,[7,8] cages at n = 17, 18,[9] fcc-like macrotetrahedron (T_d symmetry) at Au_{20},[10] tubular structures at Au_{24} and Au_{26},[8,11] fullerene-like hollow cages at Au_{32} (I_h symmetry),[5,12] tube-like cage at Au_{50} (D_{6d} symmetry),[13,14] and amorphous close-packed configurations at some medium-sized clusters such as Au_{38}, Au_{55}, etc.,[15] respectively. Meanwhile, on analogy to carbon nanotubes, single-walled gold nanotubes have been observed experimentally in electron microscope studies.[16] All of these exciting findings indicate that the structural growth sequence of Au_n clusters is rather complicated and requires very careful examinations.

So far, less attention has been paid to Au_n clusters with n = 21−30, which is believed to be a transition region from small molecule-like to nanocrystalline-like. Previously, Fa et al. predicted the existence of tubular Au_{24} and Au_{26} by density functional theory (DFT) using the DMol^3 package.[8,11] Xing et al. explored the evolution of structural motifs of gold cluster anions, Au_n^-, in the size range n = 11−24 through a comparison of electron diffraction data with DFT calculations.[17] They found that a transition from planar to three-dimensional structures in the size range of n = 12−14, cage structures for n = 16 and 17, the appearance of a tetrahedral structure at n = 20, and a tubular structure for n = 24. Zeng's and Wang's group observed the structural transitions in anionic Au_n^- (n = 21−25) clusters using photoelectron spectroscopy combined with DFT calculations,[18] and a structural transition from hollow tubular to close-packed structure is observed at n = 25. For larger Au_n clusters with $n \geq 38$, it was generally believed that the clusters mainly prefer close-packed structures of either amorphous or fcc-like type.[13,15,19] However, this structural motif might be challenged by the other motifs (like fullerene-like hollow cages) at some particular sizes. For example, a hollow C_2 cage of Au_{50} was found to be energetically favorable over the lowest-energy compact isomers.[13] Very recently, a high-symmetric tube-like D_{6d} cage was found to be even more stable than the C_2 cage.[14] Therefore, there might be a coexistence of different structural motifs in the size range of n = 21−30 for Au_n clusters. But it is unclear how those possible structural motifs (such as fcc-like, double-layered flat, hollow cage or tubular, and close-packed) compete with each other and what are the lowest-energy configurations for the neutral Au_n clusters (n = 21−30) at each size. In this paper, we address this issues by performing an extensive search on the lowest-energy structures of Au_n (n = 21−28) clusters and discuss their structural motifs and electronic properties via DFT calculations.

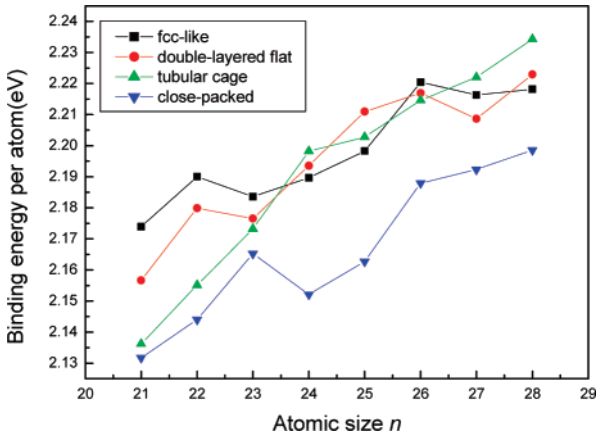

Figure 1. Binding energy per atom as a function of cluster size for the most stable fcc-like, double-layered flat, tubular cage, and close-packed isomers.

* To whom correspondence should be addressed. E-mail: tiandx@dlut.edu.cn; zhaojj@dlut.edu.cn.
† Department of Chemistry, School of Chemical Engineering.
‡ State Key Laboratory of Materials Modification by Laser, Electron, and Ion Beams, School of Physics and Optoelectronic Technology.
§ College of Advanced Science and Technology.

10.1021/jp7116938 CCC: $40.75
Published on Web 03/01/2008

TABLE 1: Symmetry, Binding Energy (E_b) per Atom, HOMO−LUMO Gap, Vertical Ionization Potential (VIP), and Average Coordination Number (CN) for Au_n (n = 21−28) Clusters

	Au_{21}	Au_{22}	Au_{23}	Au_{24}	Au_{25}	Au_{26}	Au_{27}	Au_{28}
symmetry	C_s	C_{2v}	C_s	D_{3d}	C_{2v}	C_{3v}	C_{2v}	C_{3v}
E_b (eV)	2.17	2.19	2.18	2.20	2.21	2.22	2.22	2.23
gap (eV)	0.95	0.98	0.68	0.93	0.90	0.67	0.93	0.76
VIP (eV)	6.22	6.43	6.26	6.73	6.48	6.34	6.60	6.59
CN	5.14	5.36	5.2	5.5	5.6	5.15	5.55	5.57

II. Methodological Details

To identify the lowest-energy configurations, several kinds of initial structures were generated via different approaches. First, fullerene-based hollow cages were obtained by the previously proposed capping and dualization procedures, which establish connections between carbon fullerenes and gold antifullerenes.[13,14] Second, fcc-like structures were constructed by capping adatoms on the face(s) of tetrahedral Au_{20}. Finally, close-packed configurations were obtained using genetic algorithm[20,21] with various empirical potentials.[22,23,24,25] Through these approaches, large amount of structural isomers were generated at each size, e.g., from 80 isomers for Au_{21} to 470 isomers at Au_{28}. DFT optimizations were then performed to obtain the equilibrium geometries of these isomers.

In the DFT calculations, we employed the PBE functional[26] for the exchange-correlation interaction within generalized gradient approximation (GGA) and a double numerical basis set including d-polarization functions (DNP), as implemented in DMol package.[27] A relativistic semi-core pseudopotential (DSPP) considering $5s^25p^65d^{10}6s^1$ valence electrons for Au was used in the present calculations. The accuracy of the present PBE/DNP/DSPP scheme was assessed in previous studies.[13,14] Spin-polarized GGA calculations were performed, but all Au_n isomers studied show no polarization. Normal-mode vibrational analysis was conducted to make sure that the obtained structures are real local minima rather than saddle stationary points on the potential energy surface.

III. Results and Discussion

The large amount of isomers obtained here can be grouped into a few structural growth motifs, that is, fcc-like, double-layered flat, tubular cage, and close-packed. To simplify, at each cluster size we selected the most stable configuration in each motif as representative. The structures and relative energy differences for these representative isomers of Au_n (n = 21−28) clusters are given in Figure S1 and the size-dependent binding energies for these structural motifs are compared in Figure 1. The main theoretical results from our DFT calculations are summarized in Table 1. By comparing these isomers, the lowest-energy configurations can be identified and the graphic illustration for the structural evolution of Au_n (n = 21−28) clusters are summarized in Figure 3. Within the size range studied, close-packed structural motif corresponds to the lowest binding energy, suggesting it is the least energetically favorable one among four kinds of structural motifs considered.

For Au_n (n = 21−23), fcc-like structures have the highest binding energies than the other isomers, with energy differences of at least 0.36, 0.22, and 0.16 eV, respectively. As a continuation of the magic Au_{20} cluster with extremely high stability, fcc-like configurations remain the primary growth pattern for Au_n (n = 21−23) clusters. As shown in Figure 2, the most stable configurations for Au_{21} and Au_{23} adopt fcc-like form based on a highly stable Au_{20} pyramid with one or three atoms capped on one face of Au_{20}. Although the most stable structure of Au_{22} with C_{2v} symmetry is also based on pyramid Au_{20}, the two adatoms are embedded into the tetrahedral Au_{20}.

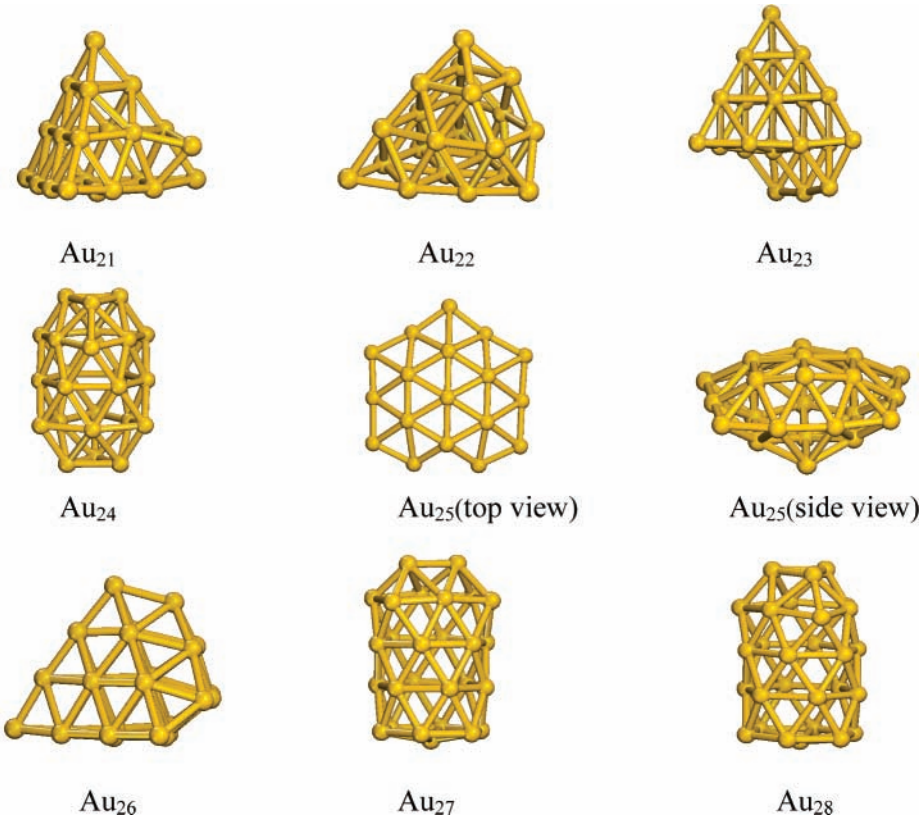

Figure 2. Graphitic illustration of structural evolution of Au_n (n = 21−28) clusters from fcc-like Au_n (n = 21−23) to tubular Au_{24} to double-layered flat Au_{25} to fcc-like Au_{26} and to tubular Au_{27} and Au_{28}. For Au_{25}, both sideview and topview are presented.

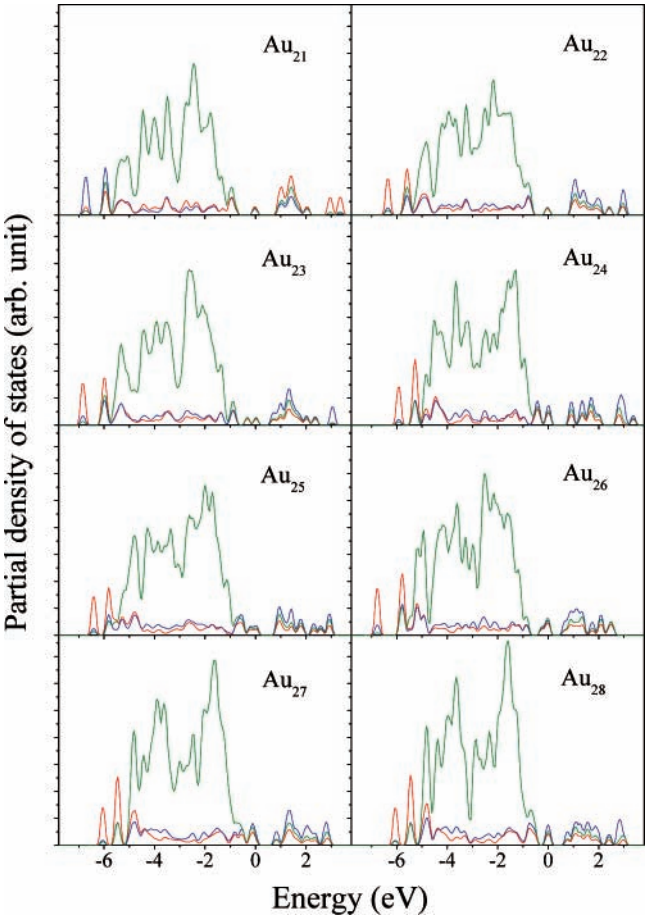

Figure 3. Partial density of states for Au_n clusters ($n = 21-28$) with their lowest-energy configurations. Fermi level is set at zero on the energy axis. Green: d states; red: s states; blue: p states.

The computed HOMO−LUMO gap reduces from 1.87 eV for Au_{20} to 0.95 eV at Au_{21}, 0.98 eV at Au_{22}, and 0.69 eV at Au_{23}. In the case of odd-sized clusters, there is no spin polarization so that both HOMO and LUMO for each cluster is half occupied. The substantial gaps found for Au_{21} and Au_{22} might be due to the extraordinarily large gap for the magic Au_{20}. Previously, Fa and Dong[8] studied the growth pattern of Au_n ($n = 21-23$) clusters and also found that pyramid-based structures are their ground states using spin-polarized relativistic all-electron DFT-GGA calculations with the same DMol package.

At $n = 24$, a tubular form with D_{3d} symmetry is the most stable one and its energy is lower than the next low-lying isomer by 0.11 eV. It is composed of three six-member rings and two capped triangles on both ends. The Au atoms in the Au_{24} cluster can be divided into two types, namely, 12 atoms with fivefold coordination and 12 atoms with sixfold coordination. The HOMO−LUMO gap of tubular Au_{24} is 0.93 eV, suggesting it is chemical inert and relatively stable. Previously, Fa et al. predicted the existence of tubular isomer by DFT calculations with GGA-PBE functional.[11] However, the tube surface of their tubular Au_{24} is distorted with a low C_2 symmetry. For comparison, the present tubular configuration has higher symmetry and its energy is 0.56 eV lower than that of the Fa's distorted tubular structure. In a recent study, the present structure was identified as the ground state of anionic Au_{24}^- by joint electron diffraction measurement and local spin-density-functional molecular dynamics simulation method with norm conserving scalar relativistic pseudopotentials.[18]

For $n = 25$, a double-layered flat form possesses the highest binding energy, and the energy differences between this lowest-energy structure and other isomers are more than 0.21 eV. The double-layered flat structure of Au_{25} might be related to the unusual stability of planar structures of smaller Au_n clusters.[6] Previous calculations predicted that Au_n ($n = 13-16$) clusters prefer similar kind of close-flat planar configurations.[7,8] However, finding such configuration in the medium-sized Au_{25} cluster is rather unexpected. The HOMO−LUMO gap of close-flat Au_{25} is 0.90 eV. In a previous combined computational study with basin-hopping algorithm and DFT (at PBE/GGA level) calculations, a pyramid-based form was reported as the lowest-energy structure,[7] which is higher by 0.5 eV in total energy than the present double-layered structure of Au_{25}.

The most stable configuration Au_{26} is fcc-like, based on a tetrahedral Au_{20} with six atoms added to one (111) face of Au_{20} pyramid. Previous theoretical work predicted that a tubular structure is the ground state of Au_{26}.[11] However, compared with present pyramid-based Au_{26}, the previously reported tubular one is higher in energy by 0.35 eV. In addition, the computed HOMO−LUMO gap of pyramid-based Au_{26} is 0.67 eV, higher than that of the tubular Au_{26} (0.40 eV).

Once again, the tubular structures with high C_{2v} and C_{3v} symmetry are the lowest-lying isomers for Au_{27} and Au_{28}, respectively. Compared with other types of isomers, tubular Au_{27}(Au_{28}) is more stable by at least 0.16 eV (0.17 eV). Their HOMO−LUMO gaps are 0.93 and 0.77 eV, respectively. Previously, Fa et al. predicted the existence of tubular Au_{27} and Au_{28}[11] and also found that tubular structures are their ground states.

The tubular Au_{24}, Au_{27}, and Au_{28} cages can be considered as capped finite gold nanotubes. Indeed, all of the three structures have identical tube sidewall, which can be obtained via dualization operation on a (6, 6) carbon nanotube,[14] while they differ in the number and configuration of capping atoms. Experimentally, single-walled gold nanotubes were reported in an electron microscope study.[16] Thus, the tubular configurations found here might be considered as embryos of the experimentally observed gold nanotubes.[16]

As shown in Table 1, the binding energy generally increases with cluster size, i.e., from 2.17 eV at $n = 21$ to $n = 2.23$ eV at $n = 28$. Thus, the clusters continue to gain energy during the growth process. The computed HOMO−LUMO gaps of Au_n clusters distribute within an energy range from 0.65 to 1.0 eV, rather insensitive to the structural motif. High VIP values (about 6.6 to 6.7 eV) were found at the tubular Au_{24}, Au_{27}, and Au_{28} clusters, which can be associated with the relatively large average coordination numbers (~5.5) of these clusters.

To further discuss the correspondence between electronic and geometry structures of these gold clusters, we have computed the partial density of states (PDOS) of Au_n clusters, as shown in Figure 3. In all the cases studied, hybridization of sp and d electrons can be observed. Careful examinations show that the PDOS exhibit distinct features for Au_n clusters belonging to different structural pattern. For example, Au_n ($n = 24$, 27, 28) with tube-like configurations possess relatively narrow d-bandwidth (about 4.0 eV), compared to the d-bandwidth of about 5.0 eV for the other clusters. Another noticeable finding is the relative location for the small DOS peak at Fermi level. For the Au_{20}-based clusters, a small peak emerge at the vicinity of Fermi level at $n = 21$ and 22, while it splits into a double peak at $n = 23$ or is broadened at $n = 26$. This single or double peak locates between the major valence bands and conduction bands. For the double-layered Au_{25}, there is also a small peak at Fermi level, which is indeed a tail of the valence band. The situation of the tube-like Au_n clusters ($n = 24$, 27, and 28) is

somewhat between the above two cases. The DOS peak at Fermi level is located at the edge of the major valence band, with very little overlap with the valence band.

IV. Summary

To conclude, four kinds of possible motifs, fcc-like, double-layered flat, tubular cage, and close-packed structures of neutral Au_n ($n = 21-28$), have been investigated by DFT calculations, and the structural evolutional sequence was summarized. It was found that Au_n ($n = 21-23$) hold fcc-like structure due to the high stability of tetrahedral Au_{20}. A structural transition from fcc-like to tubular form occurs at Au_{24}. The most stable Au_{25} is a double-layered flat structure. Again, Au_{26} prefers fcc-like structure like the smaller Au_n clusters with $n = 21-23$. For Au_{27} and Au_{28}, tubular structures dominate the low-lying isomers. The electronic properties such as VIP and PDOS show sensitivity to cluster geometry, which might be helpful for distinguishing those structural motifs experimentally. The frequent alternation of different structural motifs in the size range of $n = 21-28$ indicates strong competition between those motifs. The overall growth sequence of the medium-sized gold clusters is rather complicated and requires very careful examination. As the cluster further grows, close-packed structures would eventually become dominant for most sized clusters (with exception at some magic sizes like Au_{32} and Au_{50}). Thus, it would be interesting to reveal the transition from tubular to close-packed structures beyond $n = 28$. The research on this direction is still underway.

Acknowledgment. This work was supported by the Young Teacher Foundation of Dalian University of Technology (No. 602003), the Program for New Century Excellent Talents in University of China (NCET06-0281), the Chinese National Science Foundation (10774019), and the 973 Program (No. 2007CB613902). We thank Profs. X. C. Zeng and R. B. King for stimulating discussion and Dr. W. Fa for providing us the coordinates of Au_{26} clusters.

Supporting Information Available: Structures and relative energy differences for representative isomers of Au_n ($n = 21-28$) clusters (Figure S1). This material is available free of charge via the Internet at http://pubs.acs.org.

References and Notes

(1) Haruta, M.; Kobayashi, T.; Sano, H.; Yamada, N. *Chem. Lett.* **1987**, *2*, 405.
(2) Daniel, M. C.; Astruc, D. *Chem. Rev.* **2004**, *104*, 293.
(3) Tsoli, M.; Kuhn, H.; Brandau, W.; Esche, H.; Schmid, G. *Small* **2005**, *1*, 841.
(4) Hakkinen, H.; Moseler, M.; Landman, U. *Phys. Rev. Lett.* **2002**, *89*, 033401.
(5) Johansson, M. P.; Sundholm, D.; Vaara, J. *Angew. Chem. Int. Ed.* **2004**, *43*, 2678.
(6) Xiao, L.; Wang, L. C. *Chem. Phys. Lett.* **2004**, *392*, 452.
(7) Bulusu, S.; Zeng, X. C. *J. Chem. Phys.* **2006**, *125*, 154303.
(8) Fa, W.; Luo, C. F.; Dong, J. M. *Phys. Rev. B* **2005**, *72*, 205428.
(9) Bulusu, S.; Li, X.; Wang, L. S.; Zeng, X. C. Proc. *Natl. Acad. Sci. U.S.A.* **2006**, *103*, 8326.
(10) Li, J.; Li, X.; Zhai, H. J.; Wang, L. S. *Science* **2003**, *299*, 864.
(11) Fa, W.; Dong, J. M. *J. Chem. Phys.* **2006**, *124*, 114310.
(12) Gu, X.; Ji, M.; Wei, S. H.; Gong, X. G. *Phys. Rev. B* **2004**, *70*, 205401.
(13) Wang, J.; Jellinek, J.; Zhao, J.; Chen, Z.; King, R. B.; Schleyer, P. v. R. *J. Phys. Chem A* **2005**, *109*, 9265.
(14) Tian, D. X.; Zhao, J. J.; Wang, B. L.; King, R. B. *J. Phys. Chem.* **2007**, *A111*, 411.
(15) Garzon, I. L.; Michaelian, K.; Beltran, M. R.; Posada-Amarillas, A.; Ordejon, P.; Artacho, E.; Sanchez-Portal, D.; Soler, J. M. *Phys. Rev. Lett.* **1998**, *81*, 1600.
(16) Oshima, Y.; Onga, A.; Takayanagi, K. *Phys. Rev. Lett.* **2003**, *91*, 205503.
(17) Xing, X. P.; Yoon, B.; Landman, U.; Parks, J. H. *Phys. Rev. B* **2006**, *74*, 165423.S.
(18) Bulusu, X.; Li, L.; Wang, S.; Zeng, X. C. *J. Phys. Chem. C* **2007**, *111*, 190.
(19) Li, T. X.; Yin, S. Y.; Wang, B. L.; Wang, G. H.; Zhao, J. J. *Phys. Lett. A* **2000**, *267*, 403.
(20) Deaven, D. M.; Ho, K. M. *Phys. Rev. Lett.* **1995**, *75*, 288.
(21) Zhao, J. J.; Xie, R. H. J. *Comput. Theor. Nanosci.* **2004**, *1*, 117.
(22) Lopez, M. J.; Jellinek, J. *J. Chem. Phys.* **1999**, *110*, 8899.
(23) Sutten, A. P.; Chen, J. *Philos. Mag. Lett.* **1990**, *61*, 139.
(24) Gupta, R. P. *Phys. Rev. B* **1989**, *23*, 6265.
(25) Cleri, F.; Rosato, V. *Phys. Rev. B* **1993**, *48*, 22.
(26) Perdew, J. P.; Burke, K.; Ernzerhof, M. *Phys. Rev. Lett.* **1996**, *77*, 3865.
(27) Delley, B. *J. Chem. Phys.* **1990**, *92*, 508.